

Leakage current mechanisms of ultrathin high- κ Er₂O₃ gate dielectric film*

Wu Deqi(武德起)^{1,2,3}, Yao Jincheng(姚金城)¹, Zhao Hongsheng(赵红生)^{1,2,3},
Chang Aimin(常爱民)^{1,†}, and Li Feng(李锋)^{1,2,3}

(1 Xinjiang Technical Institute of Physics & Chemistry, Chinese Academy of Sciences, Urumqi 830011, China)

(2 Institute of Semiconductors, Chinese Academy of Sciences, Beijing 100083, China)

(3 Graduate University of the Chinese Academy of Sciences, Beijing 100049, China)

Abstract: A series of high dielectric material Er₂O₃ thin films with different thicknesses were deposited on p-type Si (100) substrate by pulse laser deposition at different temperatures. Phase structures of the films were determined by means of X-ray diffraction (XRD) and high resolution transmission electron microscopy (HRTEM). Leakage current density was measured with an HP4142B semiconductor parameter analyzer. The XRD and HRTEM results reveal that Er₂O₃ thin films deposited below 400 °C are amorphous, while films deposited from 400 to 840 °C are well crystallized with (111)-preferential crystallographic orientation. *I*-*V* curves show that, for ultrathin crystalline Er₂O₃ films, the leakage current density increases by almost one order of magnitude from 6.20×10^{-5} to 6.56×10^{-4} A/cm², when the film thickness decreases by only 1.9 nm from 5.7 to 3.8 nm. However the leakage current density of ultrathin amorphous Er₂O₃ films with a thickness of 3.8 nm is only 1.73×10^{-5} A/cm². Finally, analysis of leakage current density showed that leakage of ultrathin Er₂O₃ films at high field is mainly caused by Fowler–Nordheim tunneling, and the large leakage of ultrathin crystalline Er₂O₃ films could arise from impurity defects at the grain boundary.

Key words: Er₂O₃; high- κ gate dielectrics; leakage current; leakage current mechanisms

DOI: 10.1088/1674-4926/30/10/103003

PACC: 7755; 7360F

EEACC: 2560; 2570

1. Introduction

Up to now, SiO₂ has been the best choice for gate dielectric material, since it has excellent physical and electrical properties in MOS capacitors. MOSFET feature size has been scaling down in order to meet the low-power, high-performance requirements of CMOS circuits. The scaling of conventional gate dielectric SiO₂ is approaching its predicted limit due to large tunneling leakage current^[1]. The gate oxide leakage in SiO₂ increases exponentially with reducing physical thickness due to the tunneling effect^[2]. High dielectric constant (high- κ) materials would be potential candidates because a thicker film is utilized to reduce the leakage current while maintaining the same gate capacitance.

In order to seek suitable alternatives of SiO₂, various high- κ materials have been investigated, mainly including the metal oxides of III and IVB, such as Al₂O₃^[3–5], LaAlO₃^[5], TiO₂^[6], ZrO₂^[7–9], HfO₂^[10–12] and rare earth oxides Y₂O₃^[13,14], La₂O₃^[15], Pr₂O₃^[16]. Amorphous materials are mostly selected as gate dielectrics because leakage current can be formed at the grain boundary in polycrystalline materials of high dielectric oxides. Furthermore, amorphous gate dielectric materials possess the virtues of easy preparation, good reproducibility, and could be compatible with the traditional production process. Thus, they have been widely

studied by researchers. Unfortunately, most amorphous materials of high dielectric oxides tend to re-crystallize after annealing, causing high leakage current at the grain boundary. Though single crystal materials of high dielectric oxides have no grain boundary and little leakage current in theory, they are difficult to prepare. So we hope to clarify the leakage current mechanisms of high- κ gate dielectric films. High- κ material Er₂O₃ is the only stable oxide of erbium on the earth with a large conduction band offset (~ 3.5 eV) and a wide band gap (~ 7.6 eV)^[17]. Er₂O₃ has a complex bixbyite cubic structure with a lattice constant of 1.054 nm, which is nearly twice the lattice constant of Si. Er₂O₃ has become a potential high- κ gate dielectric material because the lattice mismatch on Si is less than 3%, and it is easy to form films with preferential crystallographic orientation on Si; in addition, it possesses good thermal stability on Si^[18]. Polycrystalline high- κ gate dielectric Er₂O₃ films have been deposited on Si by several groups in recent years^[19–22]. Epitaxial growth of Er₂O₃ films on Si (100) has been realized through molecular beam epitaxy (MBE) by Chen^[23] and Xu^[24]. However, leakage current mechanisms of gate dielectric Er₂O₃ thin films have merely been reported. In this work, we explore the preparation methods of ultrathin amorphous/polycrystalline Er₂O₃ gate dielectric films on p-type Si (100) by pulse laser deposition (PLD) through ablating Er₂O₃ ceramic target under high-vacuum conditions.

* Project supported by the Knowledge Innovation Program of the Chinese Academy of Sciences (No. 072C201301) and the Graduate Student Innovation Program of the Chinese Academy of Sciences.

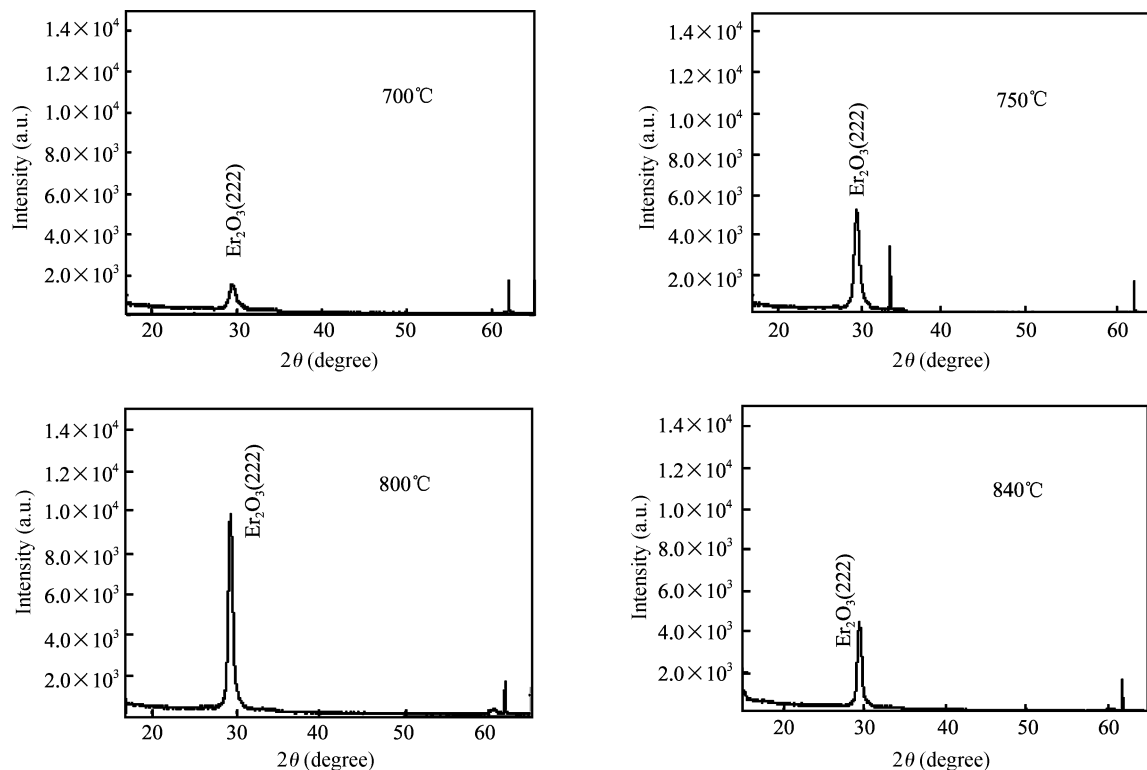
† Corresponding author. Email: changam@ms.xjb.ac.cn

Received 18 May 2009, revised manuscript received 31 May 2009

© 2009 Chinese Institute of Electronics

Table 1. Deposition conditions of Er_2O_3 thin films by PLD.

Parameter	Value
Target	Er_2O_3 ceramic target
Base vacuum pressure	2×10^{-6} Pa
Substrate	p-type Si (001)
Substrate temperature	25, 200, 400, 500, 700, 750, 800, 840 °C
Gas pressure	no
Repetition frequency	1 Hz
Power density	3.75 J/cm^2
Target-substrate distance	8 cm

Fig. 1. XRD of Er_2O_3 thin films deposited at different temperatures.

Meanwhile, the effects of deposition temperature on the phase structure and morphology of Er_2O_3 films, as well as the effects of film thickness and phase structure on leakage current of ultrathin Er_2O_3 gate dielectric films have been investigated.

2. Experiments

P-type Si (100) with a resistivity of 8–12 $\Omega\cdot\text{cm}$ was selected as the substrate. After being pretreated by the standard semiconductor cleaning process and dried with nitrogen, the sample was immediately loaded into the deposition chamber of the PLD equipment. A Lambda Physik KrF laser (248 nm wavelength and 25 ns pulse duration) was focused on the target at an angle of 45 degrees. Er_2O_3 with a purity of 99.95% was used as the target. The target and the substrate were kept rotating in order to ensure the uniformity of Er_2O_3 films during deposition. Er_2O_3 films were deposited at 25, 200, 400, 500, 700, 750, 800 and 840 °C respectively, as shown in Table 1. Circular aluminum pads with areas of $5.54 \times 10^{-3} \text{ cm}^2$ were defined as the top electrodes for the MOS capacitor through stan-

dard photolithography, aluminum deposition, and wet chemical etching techniques. In addition, the back side of the silicon wafer was cleaned, on which a 100-nm-thick aluminum film was deposited to facilitate Ohmic contact for vertical measurements. Phase structure characterization of the samples was carried out by X-ray diffraction (XRD) and high-resolution transmission electron microscopy (HRTEM), and the surface morphology was determined by atomic force microscopy (AFM). Furthermore, the current–voltage (I – V) characteristics of the MOS capacitors were vertically measured by an HP 4142B semiconductor parameter analyzer.

3. Results and discussion

XRD spectra of those films deposited at 700, 750, 800 and 840 °C are shown in Fig. 1. No peak is observed on the curves of Er_2O_3 thin films deposited below 400 °C, and the diffraction peaks of the film deposited at 400 °C are not obvious.

The peak of Er_2O_3 (222) is obvious on the curves of

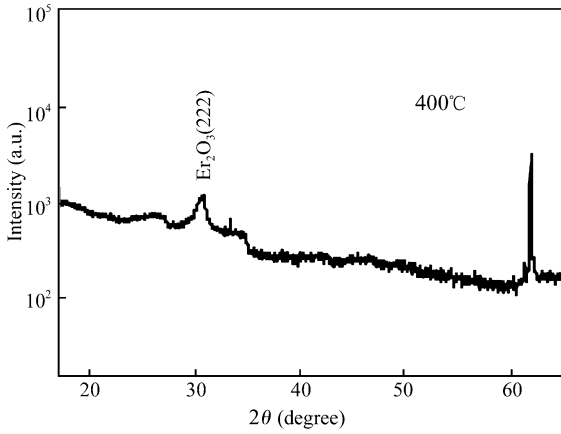


Fig. 2. XRD of Er_2O_3 thin film deposited at 400 °C.

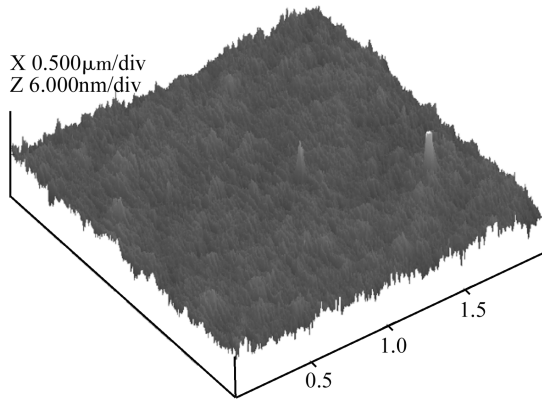


Fig. 3. Surface morphology of the $\text{Er}_2\text{O}_3/\text{a-Ni-Al-O}$ stack.

Er_2O_3 thin films deposited above 400 °C, and there is a weak peak of Er_2O_3 (444) at $2\theta = 60.8^\circ$ on the curves of Er_2O_3 thin films deposited from 700 to 840 °C. Based on the observed results, it could be concluded that Er_2O_3 thin films deposited from 400 to 840 °C have been well crystallized with (111)-preferential crystallographic orientation, while the films deposited below 400 °C are amorphous.

It has been found that the peaks of Er_2O_3 (222) on the curves of Er_2O_3 thin films deposited at 400, 750, 800 and 840 °C are strengthened after annealing in oxygen ambience at 450 °C for 60 min, but the weak peaks of Er_2O_3 (444) still exist. This indicates that annealing is propitious to preferential crystallographic orientation. The weak peaks of Er_2O_3 (222) on the curves of post-annealed Er_2O_3 thin films deposited at 400 °C can be clearly observed by using logarithmic coordinates, as shown in Fig. 2. This shows that the films crystallized with poor orientation due to low annealing temperature. No peak has been observed on the curves of Er_2O_3 thin films deposited below 400 °C, which indicates that depositing temperature is not high enough for thin films to crystallize.

The electrical properties of MOS capacitor can be directly affected by the sample surface morphology. The surface of Er_2O_3 thin film is atomically sharp with a root-mean-square roughness (RMS) of 0.591 nm, as shown in Fig. 3.

Texture could be clearly observed on the HRTEM image of ultrathin crystalline Er_2O_3 high- κ gate dielectric film, as shown in Fig. 4. The inconsistent orientation of the stripe

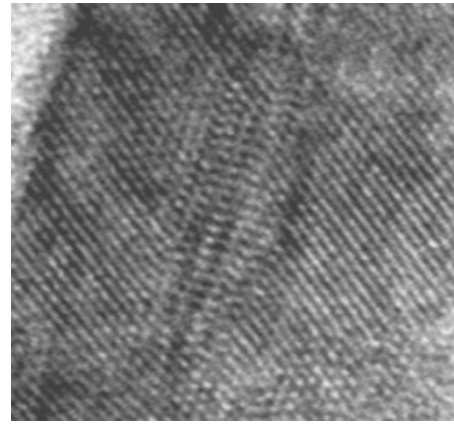


Fig. 4. HRTEM image of ultrathin Er_2O_3 film deposited at 700 °C.

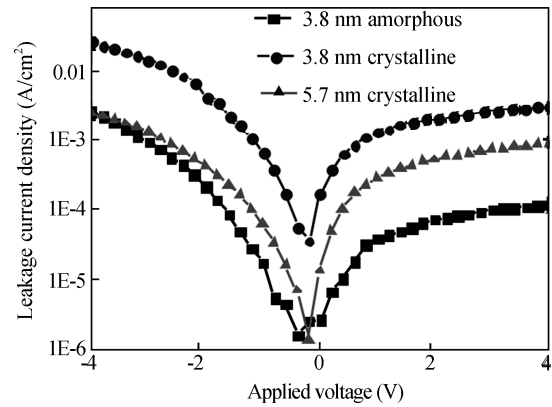


Fig. 5. I - V curves of crystalline/amorphous Er_2O_3 films with different thicknesses.

Table 2. Leakage current density of Er_2O_3 film with various thicknesses measured at -1 V bias.

Er_2O_3 thin film	Leakage current (A/cm^2)
5.7 nm crystalline	6.20×10^{-5}
3.8 nm crystalline	6.56×10^{-4}
3.8 nm amorphous	1.73×10^{-5}

texture indicates that the crystalline Er_2O_3 film is polycrystalline.

The leakage current density is not a serious problem for relatively thick films^[25] given that the leakage current density is inversely proportional to the thickness of the high- κ dielectric film, if the applied electric field is not too high. Nevertheless, there is a sharp increase when the thickness of the film is less than 5 nm for crystalline Er_2O_3 films. Once the thickness is below this value, a substantial increase of leakage current density can be observed, as illustrated in Fig. 5. Table 2 summarizes the leakage current density at -1 V bias for these samples. It can be seen that the leakage current density of crystalline Er_2O_3 film increases by one order of magnitude from 6.20×10^{-5} to 6.56×10^{-4} A/cm^2 for a decrease in the film thickness of only 1.9 nm from 5.7 to 3.8 nm.

The leakage current not only varies with the thickness of crystalline films, but also depends on the phase structure of the films with similar thickness, as shown in Table 2 and Fig. 5. For the 3.8 nm amorphous Er_2O_3 thin film, the leakage current density is as low as 1.73×10^{-5} A/cm^2 , almost 38

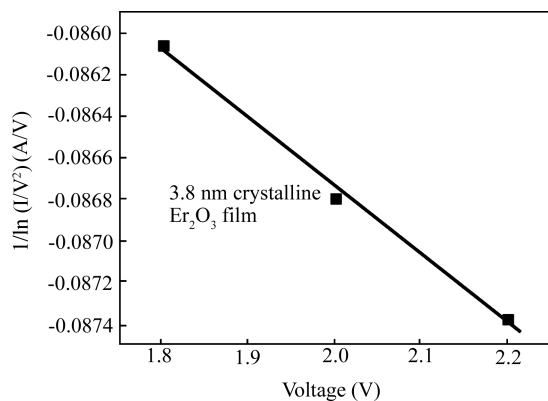


Fig. 6. High field Fowler-Nordheim plot of 3.8 nm crystalline Er_2O_3 film.

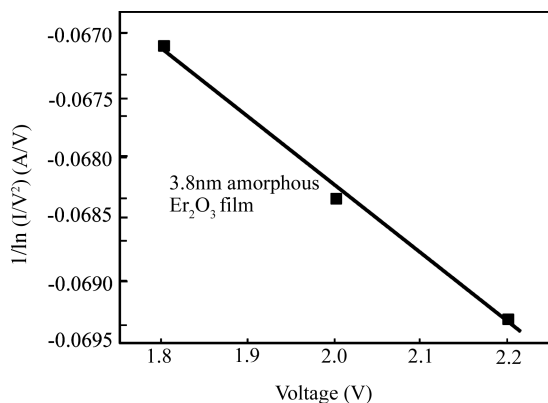


Fig. 7. High field Fowler-Nordheim plot of 3.8 nm amorphous Er_2O_3 film.

times lower than that of 3.8 nm crystalline films. This contradicts the result reported by Guha *et al.*^[25] on aluminum oxide films, since there were no leakage current density differences between amorphous and crystalline phases. Considering the interfacial layer of the 3.8 nm Er_2O_3 samples, the calculated equivalent oxide thickness (EOT) of this sample is only ~ 1.3 nm. Typical leakage current density for 1.3 nm silicon dioxide is higher than 10 A/cm^2 ^[26], six orders of magnitude higher than the amorphous Er_2O_3 films with the same EOT in this study. It is worth mentioning that the leakage current of the 3.8 nm ultrathin amorphous Er_2O_3 film is lower than that of 5.7 nm crystalline Er_2O_3 film.

There is a substantial difference of leakage current density between amorphous and crystalline Er_2O_3 film. Direct tunneling is initially considered as the most likely mechanism which could cause high leakage in ultrathin dielectric films. The thickness of Er_2O_3 films being investigated is more than 3.5 nm. Considering the interfacial layer of 0.6 nm, the physical thickness of the whole thin film stacks is at least 4 nm. In order to determine the possible causes of the substantial leakage current difference between ultrathin amorphous and crystalline Er_2O_3 films, the I - V curves from low field to high field are plotted for 3.8 nm amorphous/crystalline Er_2O_3 films, as shown in Figs. 6–9.

Tunneling either happens at high electric field ($> 4 \text{ MV/cm}$) or occurs for films less than 3 nm at low field^[27]. The F–N plots (Figs. 6, 7) of both ultrathin crystalline and amor-

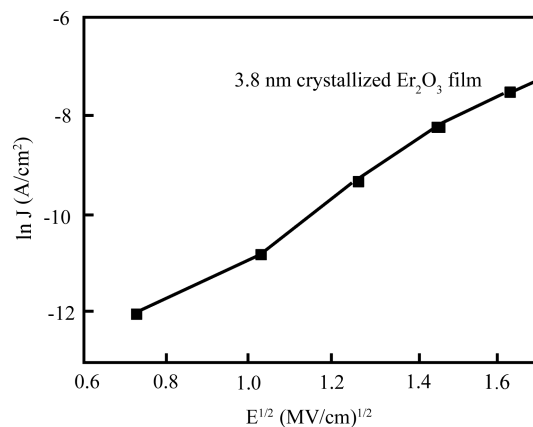


Fig. 8. Schottky emission plot of 3.8 nm crystalline Er_2O_3 film.

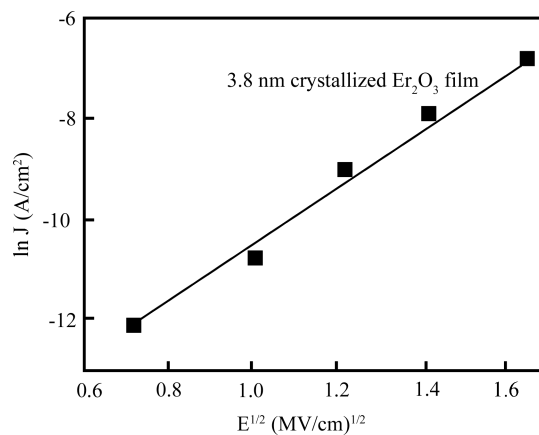


Fig. 9. Schottky emission plot of 3.8 nm amorphous Er_2O_3 film.

phous Er_2O_3 have revealed that the dominant leakage at high field is from Fowler–Nordheim tunneling. F–N tunneling does not coexist with direct tunneling, so the possibility of direct tunneling in these films can be ruled out.

As the sample was not shielded during the test, the weak signal at low electric field tends to wobble, which may be induced by interference of the electromagnetic signal outside, so Ohmic plots of the Er_2O_3 films could not be obtained.

The main difference between amorphous and polycrystalline Er_2O_3 film is that there are grain boundaries in crystalline Er_2O_3 films. Grain boundaries have been believed not only to be a site where defects and impurities prefer to aggregate, but also may act as a fast diffusion path for boron dopants in the p-type substrate. It has been reported that oxygen diffusion is 5–6 orders of magnitude faster along the grain boundary of ZrO_2 films than in the bulk^[28]. The concentration of boron at the grain boundaries of high- κ Er_2O_3 films will lead to an increase in leakage current.

As mentioned above, the difference of leakage current density between crystalline and amorphous Er_2O_3 films may be caused by the grain boundaries. For crystalline Er_2O_3 films, the distance which carriers travel is proportional to the total length of grain boundaries, while the total length of grain boundaries is approximately equal to the thickness of ultrathin Er_2O_3 films. Therefore, the leakage current density should be inversely proportional to the thickness, if the resistivity of grain boundaries is uniform. In other words, leakage current

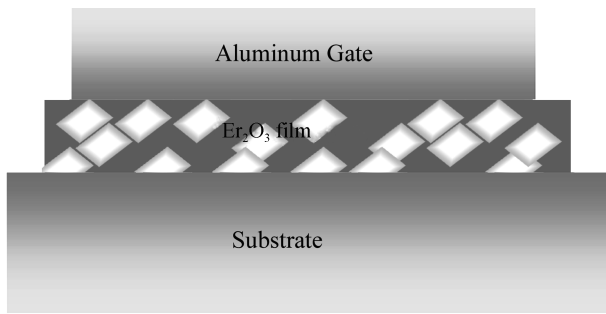


Fig. 10. Sketch of a cross-sectional view of a capacitor^[33]. The metal tips are formed at the interface between the aluminum gate and Er_2O_3 film.

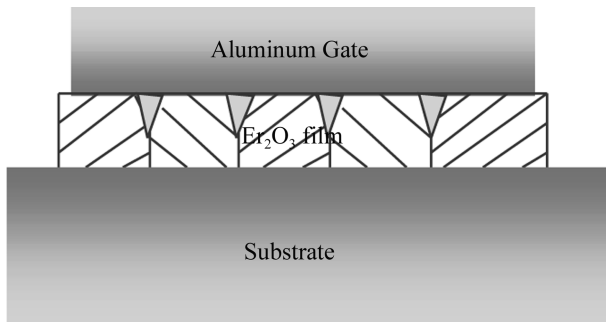


Fig. 11. Sketch of a cross-sectional view of a capacitor. The grain boundaries of the crystalline Er_2O_3 film are represented by small blocks with inclined lines of different directions^[33].

density through crystalline films with different thicknesses, at the same low electrical field, should be of the same order of magnitude if other conduction mechanisms can be neglected. Unfortunately, the above hypothesis is untenable, since an obvious span of leakage current exists when the crystalline Er_2O_3 film thickness is about 5 nm.

In order to ascertain the reason for the obvious span of leakage current when the crystalline Er_2O_3 film thickness is about 5 nm, we review the cross-sectional morphology of crystalline Er_2O_3 ultrathin film, as shown in Fig. 4. Small crystallites may be clearly identified on the HRTEM image, and grains are randomly distributed. It can be imagined that electrons will go straight across the film if it is very thin, while electrons will go a roundabout way in a relative thick film.

Sketch maps are plotted, as shown in Figs. 10 and 11, so as to further ascertain the morphology difference between ultrathin and relatively thick Er_2O_3 films. The aluminum gate electrode and silicon substrate are shown to demonstrate the actual MOS structure as well as the leakage current path through grain boundaries. As shown in Fig. 11, the grain boundaries go straight through the layer in the thinner film. However, they have a zigzag path through the thicker crystalline films, as shown in Fig. 10. Adjacent grains are connected by a “line”, while three grains form a “ Λ ” type connection. Both the “line” and the “ Λ ” type connection have been reported to be responsible for leakage in crystalline high- κ films^[29]. The leakage current density has been considered to be proportional to the total length of the grain boundary in crystalline Ta_2O_5 films^[30]. The “ Λ ” type connection is the

dominant factor in the high leakage in HfO_2 films^[31]. Given that both types of boundaries are beneficial to large leakage formation, electrons need to pass through several grain boundaries from the top electrode to the substrate in relatively thick films. It is difficult for electrons to pass through certain dielectric film if the grain boundaries have bulk properties. For ultrathin crystalline films as illustrated in Fig. 11, the grains are distributed in two dimensions. The “ Λ ” type connections form a path from the top aluminum electrode to the substrate. To make matters worse, aluminum could adhere well to high- κ film after post metal deposition annealing. Aluminum atoms may subsequently diffuse along the “line” and the “ Λ ” type connection, similar to boron penetration into high- κ films^[32]. This could cause a sharp aluminum tip of a few angstroms at the top electrode. When electrical field is applied, the electric field at the sharp tip is enhanced; consequently, the metal tip may emit electrons very efficiently, and the emitted electrons may directly pass through the “ Λ ” type connection. Based on the analysis of leakage current, it has been found that the distribution of the “ Λ ” type connection is uniform in the films and each “ Λ ” type connection may contribute equally to the leakage current.

Based on the understanding of the “ Λ ” type connection and metal tip, we can explain the differences of Schottky plots between amorphous and crystalline Er_2O_3 ultrathin films, as shown in Figs. 8 and 9. For amorphous films, the interface between the film and electrode is flat, because there are no “ Λ ” type connections or “line” grain boundaries. Thus, the contact of these two materials will form an ideal energy barrier. However, under high field bias, it is not the same at those points where “ Λ ” type connections exist in ultrathin crystalline films. So the Schottky plot is non-linear in ultrathin crystalline films as shown in Fig. 8.

4. Conclusion

Er_2O_3 thin films have been deposited on p-type Si (100) by PLD. Er_2O_3 thin films deposited below 400 °C have been found to be amorphous, while those deposited from 400 to 840 °C are well crystallized with (111)-preferential crystallographic orientation. The leakage current density shows a sharp increase when the thickness of crystalline Er_2O_3 thin films decreases below 5 nm. The leakage current density increases from 6.20×10^{-5} to 6.56×10^{-4} A/cm², when the thickness is reduced from 5.7 to 3.8 nm. Nevertheless, the leakage current density of amorphous Er_2O_3 thin films with thicknesses below 5 nm still remains small; it is only 1.73×10^{-5} A/cm² for a 3.8-nm-thickness amorphous Er_2O_3 thin film, almost 38 times lower than that of 3.8 nm crystalline Er_2O_3 thin films. Leakage of the ultrathin Er_2O_3 film at high field could be mainly caused by Fowler–Nordheim tunneling, and the large leakage of the ultrathin crystalline Er_2O_3 film is probably a result of impurity defects at the grain boundaries. The leakage current at high field is amplified due to the diffusion of metal-electrode atoms along grain boundaries.

References

- [1] Muller D A, Sorsch T, Moccio S, et al. The electronic structure at the atomic scale of ultrathin gate oxides. *Nature*, 1999, 399: 758
- [2] Lo S H, Buchanan D A, Taur Y, et al. Quantum-mechanical modeling of electron tunneling current from the inversion layer of ultra-thin-oxide nMOSFET's. *IEEE Electron Device Lett*, 1997, 18(5): 209
- [3] Gusev E P, Copel M, Cartier E, et al. High-resolution depth profiling in ultrathin Al₂O₃ films on Si. *Appl Phys Lett*, 2000, 76(2): 176
- [4] Klein T M, Niu D, Epling W S, et al. Evidence of aluminum silicate formation during chemical vapor deposition of amorphous Al₂O₃ thin films on Si (100). *Appl Phys Lett*, 1999, 75(25): 4001
- [5] Wang D S, Yu T, You B, et al. Properties of high- κ gate dielectric LaAlO₃ thin films. *Journal of Inorganic Materials*, 2003, 18(1): 229
- [6] Meng L J, Teixeira V, Cui H N, et al. A study of the optical properties of titanium oxide films prepared by dc reactive magnetron sputtering. *Appl Surf Sci*, 2006, 252(22): 7970
- [7] Zhang R, Zhang X, Hu S. Nanocrystalline ZrO₂ thin films as electrode materials using in high temperature-pressure chemical sensors. *Mater Lett*, 2006, 60: 3170
- [8] Sayan S, Nguyen N V, Ehrstein J, et al. Structural, electronic, and dielectric properties of ultrathin zirconia films on silicon. *Appl Phys Lett*, 2005, 86(15): 152902
- [9] Zhu L Q, Fang Q, He G, et al. Microstructure and optical properties of ultra thin Zirconia films prepared by nitrogen assisted reactive magnetron sputtering. *Nanotechnol*, 2005, 16: 2865
- [10] Takanori M, Makoto F, Rafael R M, et al. HfO₂ thin films prepared by ion beam assisted deposition. *Surface and Coatings Technology*, 2003, 169/170: 528
- [11] Yan Z J, Xu R, Wang Y Y, et al. Thin HfO₂ films grown on Si(100) by atomic oxygen assisted molecular beam epitaxy. *Appl Phys Lett*, 2004, 85(1): 85
- [12] Harris H, Choi K, Mehta N, et al. HfO₂ gate dielectric with 0.5 nm equivalent oxide thickness. *Appl Phys Lett*, 2002, 81(6): 1065
- [13] Hunter M E, Reed M J, El-Masry N A, et al. Epitaxial Y₂O₃ films grown on Si(111) by pulsed-laser ablation. *Appl Phys Lett*, 2000, 76(14): 1935
- [14] Ioannou-Sougleridis V, Vellianitis G, Dimoulas A. Electrical properties of Y₂O₃ high-dielectric gate dielectric on Si (001): the influence of postmetallization annealing. *J Appl Phys*, 2003, 93(7): 3982
- [15] Lippert G, Dabrowski J, Melnik V, et al. Si Segregation into Pr₂O₃ and La₂O₃ high- κ gate oxides. *Appl Phys Lett*, 2005, 86(14): 042902
- [16] Nigro R L, Toro R G, Maladrino G, et al. A simple route to the synthesis of Pr₂₃ high- κ films. *Adv Mater*, 2003, 15(13): 1071
- [17] Zhu Y Y, Chen S, Xu R, et al. Band offsets of Er₂O₃ films epitaxially grown on Si substrates. *Appl Phys Lett*, 2006, 88(16): 162909
- [18] Ono H, Katsumata T. Interfacial reactions between thin rare-earth-metal oxide films and Si substrates. *Appl Phys Lett*, 2001, 78(13): 1832
- [19] Singh M P, Thakur C S, Shalini K, et al. Structural and electrical characterization of erbium oxide films grown on Si(100) by low-pressure metalorganic chemical vapor deposition. *Appl Phys Lett*, 2003, 83: 2889
- [20] Mikhelashvili V, Eisenstein G, Edelmann F. Structural properties and electrical characteristics of electron-beam gun evaporated erbium oxide films. *Appl Phys Lett*, 2002, 80(12): 2156
- [21] Mikhelashvili V, Eisenstein G, Edelmann F, et al. Characteristics of electron-beam-gun-evaporated Er₂O₃ thin films as gate dielectrics for silicon. *J Appl Phys*, 2001, 90(10): 5447
- [22] Mikhelashvili V, Eisenstein G, Edelmann F, et al. Structural and electrical properties of electron beam gun evaporated Er₂O₃ insulator thin films. *J Appl Phys*, 2004, 95(2): 613
- [23] Chen S, Zhu Y Y, Xu R, et al. Superior electrical properties of crystalline Er₂O₃ films epitaxially grown on Si substrates. *Appl Phys Lett*, 2006, 88(22): 222902
- [24] Xu R, Zhu Y Y, Chen S, et al. Epitaxial growth of Er₂O₃ films on Si (001). *J Cryst Growth*, 2005, 277(1-4): 496
- [25] Guha S, Cartier E, Gribelyuk M A, et al. Atomic beam deposition of lanthanum and yttrium based oxide thin films for gate dielectrics. *Appl Phys Lett*, 2000, 77(17): 2710
- [26] Hirose M, Koh M, Mizubayashi W, et al. Fundamental limit of gate oxide thickness scaling in advanced MOSFETs. *Semicond Sci Technol*, 2000, 15: 485
- [27] Schnupp P. A δ -well model for solid-state tunneling. *Solid-State Electron*, 1967, 10(8): 785
- [28] Wong H, Iwai H. On the scaling issues and high- κ replacement of ultrathin gate dielectrics for nanoscale MOS transistors. *Microelectron Eng*, 2006, 83(10): 1867
- [29] Naoki K, Kiyoshi O, Ryoichi F, et al. Characterization of Ta₂O₅ thin films with small current leakage for high density DRAMs. *Structure and Electronic Properties of Ultrathin Dielectric Films on Silicon and Related Structures*, Nov 29-Dec 1 1999. 2000. Boston, MA, USA: Materials Research Society, Warrendale, PA, USA
- [30] Lee J S, Joo S K. The problems originating from the grain boundaries in dielectric storage capacitors. *Solid-State Electron*, 2002, 46(10): 1651
- [31] Ikeda H, Goto T, Sakashita M, et al. Local leakage current of HfO₂ thin films characterized by conducting atomic force microscopy. *Jpn J Appl Phys*, 2003, 42(4B): 1949
- [32] Liu C L. Modelling investigation of boron diffusion in polycrystalline HfO₂ films. *Diffusion and Defect Data, Part A: Defect and Diffusion Forum*, 2002, 206/207: 123
- [33] Gao Y. Deposition, Stabilization and characterization of ZrO₂ and HfO₂ thin films for high- κ gate dielectrics. PhD Thesis, University of Arizona, Ann Arbor, 2004